



# Image registration between MRI and spot mammograms for X-ray guided stereotactic breast biopsy: preliminary results

S. Said<sup>a</sup>, P. Clauser<sup>b</sup>, N.V. Ruiter<sup>a</sup>, P.A.T. Baltzer<sup>b</sup>, and T. Hopp<sup>a</sup>

<sup>a</sup>Karlsruhe Institute of Technology (KIT), Institute for Data Processing and Electronics,  
Karlsruhe, Germany

<sup>b</sup>Medical University of Vienna, Department of Biomedical Imaging and Image-guided Therapy,  
Vienna, Austria

## ABSTRACT

Breast cancer is the most common cancer type among women. Approximately 40,000 women are expected to die from breast cancer every year. While digital mammography has a central role in the early diagnosis of breast cancer, many cancers are not visible in mammography, for example in women with dense breast tissue. Contrast enhanced magnetic resonance imaging (CE-MRI) of the breast is often used to detect lesions not visible in mammography. Lesions with suspicious characteristics on CE-MRI need to be further assessed with MRI-guided biopsy. However, MRI-guided biopsy is expensive, time consuming, and not widely available. In this paper, a novel method for a matching tool between MRI and spot mammograms is proposed. Our aim is to transfer information that is only visible in MRI onto mammographic spot projections, to enable X-ray guided biopsy even if the lesion is only visible in MRI. Two methods of registration in combination are used; a biomechanical model based registration between MRI and full view X-ray mammograms and a subsequent image based registration between full mammograms and spot mammograms. Preliminary results assessed for one patient from the Medical University of Vienna are presented. The target registration error (TRE) of biomechanical model based registration is 2.4 mm and the TRE of the image based registration is 9.5 mm. The total TRE of the two steps is 7.3 mm.

**Keywords:** Biomechanical Model Based Registration, Image Based Registration, Magnetic Resonance Imaging, Full Mammograms, Spot Mammograms

## 1. INTRODUCTION

Breast cancer is the most frequent cancer among women<sup>1,2</sup> It affects 2.1 million women each year. Despite the improvements in diagnosis and therapy, breast cancer also remains one of the leading causes of cancer-related deaths. In 2018, 15% of all cancer deaths were caused by breast cancer.<sup>3</sup> Magnetic resonance imaging (MRI) may detect additional lesions which are not visible when using conventional imaging methods such as X-ray mammography or ultrasound.<sup>4</sup> Depending on the degree of suspicion, these lesions may be either followed up or a biopsy is required.<sup>5</sup> While ultrasound can be used to identify and biopsy the suspicious lesion identified by MRI, in some cases no correlate can be identified on ultrasound and an MRI-guided biopsy is needed.<sup>6</sup> Therefore, for lesions that cannot be identified by ultrasound nor X-ray mammography, MRI-guided breast interventions remain crucial. MRI-guided biopsies, however, are expensive and a recent survey has identified a significant shortage of facilities that can perform MRI-guided breast interventions in European countries as well as in other countries.<sup>7</sup> Without them, MRI findings cannot be translated into a clinical workflow. That is why a lack of MRI-guided breast interventions is considered a serious problem.<sup>8</sup>

In this paper a new approach for a clinical workflow is proposed as shown in Figure 1: instead of using MRI-guided biopsy, the position of a lesion visible only in MRI will be transferred to X-ray guided biopsy by a model based image registration, allowing an X-ray guided lesion workup. First, the lesion detected by MRI is aligned with the full X-ray mammogram using a biomechanical model based registration. Our method originates from our earlier work.<sup>9</sup> It has been applied in an automated registration workflow and tested with clinical datasets<sup>1,10</sup> Second, the localization of the lesion in the full mammogram is transferred to the spot mammogram, which is taken during X-ray guided biopsy, using an image based registration. In this work, we apply our method to images from an X-ray guided biopsy device from Fischer Imaging Corp., in which the patient lies prone.<sup>11</sup>

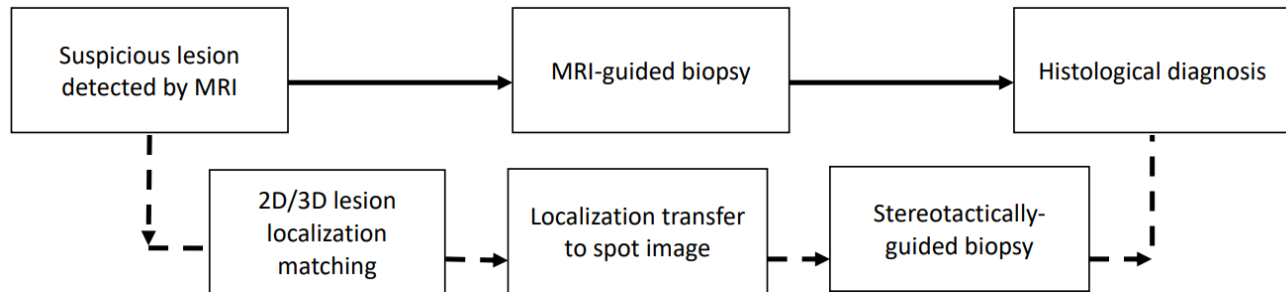


Figure 1. Suspicious breast lesions detected by MRI. Top row/solid lines: traditional workflow using costly MRI-guided biopsy. Bottom row/dashed lines: proposed new workflow by image registration.

In this paper, we focus on presenting the basic methods to use X-ray guided biopsy instead of MRI-guided biopsy for a clinical workflow. We also discuss the methods of image registration, which have been developed. We present preliminary results with a clinical dataset regarding this workflow.

## 2. METHODS

The general idea of this work is establishing a registration method between MRI and spot mammogram images taken during X-ray guided biopsy. It consists of two steps of image registration as shown in Figure 4, involving three modalities. Each modality images the breast in a different configuration. For MRI images, 3D images in prone position are acquired with the breast subject to gravity. For full mammograms, a 2D image of the patient in the upright standing position is acquired, while the breast is compressed between two parallel compression plates. A small burst of X-rays is produced from the machine passing through the breast to a detector positioned at the opposite side. For spot mammograms, a 2D image of size  $50 \times 50$  mm with a detailed view of the compressed breast is taken in prone position in devices of e.g. Fischer and Lorad. In this paper the spot mammograms in the clinical workflow are taken using a Fischer table. For keeping the lesion in a fixed position during the procedure, the breast is compressed between two plates. Once the lesion is properly detected, a pair of images is taken after moving the X-ray tube and the detector assembly  $+15^\circ$  and  $-15^\circ$  relative to the  $0^\circ$  position.<sup>11</sup>

### 2.1 Biomechanical model based registration

First, we developed a method for MRI to full X-ray mammography registration.<sup>10</sup> It uses the breast geometry as imaged with MRI in 3D to estimate a configuration of the breast that is comparable to its shape in X-ray mammography. The deformation applied virtually to the MRI is simulated by a biomechanical model.

For obtaining the patient specific breast geometry, we mainly concentrate on image segmentation for three tissues: fatty, glandular, and muscle tissues. Our implementation uses Fuzzy C-means<sup>12</sup> and K-means<sup>13</sup> clustering of the image intensities. If available, the information of the tissues imaged with different MRI protocols can be combined. For simplicity, we model the shape of the breast until a certain offset after the sternum position in posterior direction. Based on the segmented MRI, the model geometry is generated, dividing the breast anatomy into approximately 2000  $\sim$  2500 4-node elements using a tetrahedral meshing algorithm. The meshing algorithm first divides the outer and inner surfaces of the breast tissues into a triangular mesh based on the Delaunay triangulation.<sup>14</sup> Afterwards the volumetric mesh is filled with tetrahedrons in-between. Each element of the mesh is assigned to tissue-specific material properties according to the labels of regions produced by the meshing algorithm. We are applying an isotropic hyperelastic neo-hookean material model<sup>15</sup> to account for nonlinear and incompressible tissue behaviour during the deformation process for the breast. It is determined by two material constants  $C_{01}$  and  $D_1$ , as a function of Young's modulus  $E$  and Poisson's ratio  $\nu$ . The incompressibility for the model is approximated by assuming  $\nu = 0.495$  for all of the three tissues. Additionally, the Young's modulus is assumed to be 1100 Pa for the fatty tissue, 2500 Pa for the glandular tissue and 6000 Pa for the muscle tissue which is in the same range of our previous work.<sup>16</sup> Our simulation is started using these empiric standard parameters.

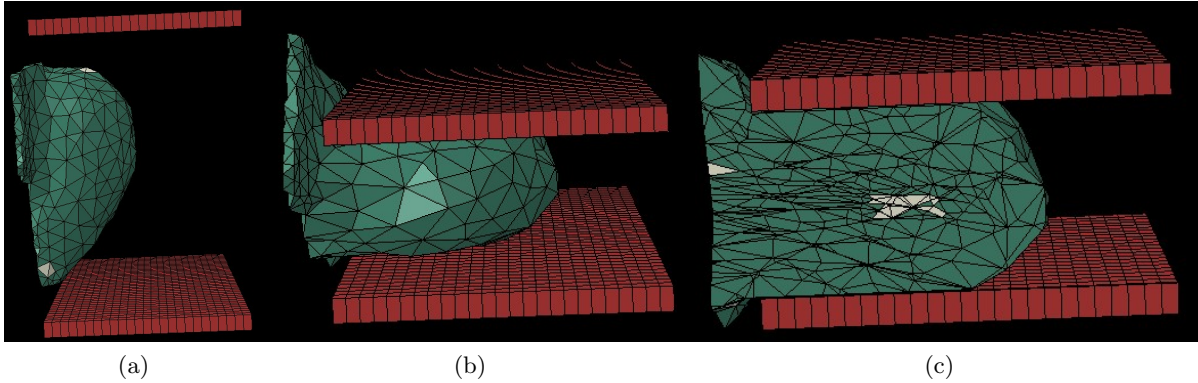


Figure 2. Schematic of the breast geometry in the biomechanical simulation before deformation (a). Schematic of the breast deformed after applying the compression plates (b). Schematic of the inner distribution of tissues showing fatty (green) and glandular tissue (white) in the compressed breast (c).

In posterior direction we model the fixation of the breast at the chest wall. In terms of boundary conditions, the breast is attached to the body by modeling the muscle as an undeformable body. Nodes at the interface between the muscle and other tissue are restricted in moving in anteroposterior direction.

The deformation simulation for the mammographic compression consists of two steps. We first estimate the breast in an unloaded state, i.e. in a configuration in which no mechanical deformation and no gravity is applied to the breast. Secondly, we add compression plates to simulate the mammographic compression. We fix the lower compression plate at the inframammary fold and then move the upper plate downwards to compress the breast until the desired compression thickness is reached as shown in Figure 2. The boundary condition is thereby defined as a displacement of the compression plates. We use acrylic glass plates modeled by 8-node hexahedrons. The compression thickness is read out from the mammogram meta data. The compression of the breast model is achieved by defining a contact between the breast surface and the plate surface. Since the material is considered nearly incompressible, the applied deformation results mostly in a change of shape and not in a change of volume.

We use the Finite Element Method (FEM) to solve the mechanical deformation problem. The mechanical deformations are computed using the dynamic FE solver in the commercial FEM software ABAQUS.<sup>17</sup>

After the deformation simulation, the deformation field is applied to the segmented MRI image, resulting in a volume containing the deformed configuration of the breast. The deformed MRI volume is calculated by linear interpolation of the deformation field at all voxels and bilinear interpolation of the voxel intensities. This volume serves as basis to carry out an X-ray-like projection. A raycasting algorithm is applied for this purpose. We take into consideration the geometry of the X-ray acquisition process using the available information from the meta data such as source to detector distance, source to patient distance, and compression thickness.

We optimize the biomechanical model based registration in order to adapt it to patient specific characteristics and uncertainties in the meta data. For this purpose we optimize a number of parameters, such as the compression thickness from the mammogram’s meta data which might have an error in the range of 5 mm,<sup>18</sup> the Young’s modulus of fatty and glandular tissue, the positioning of the compression plate and a possible patient rotation around the three main axes. Optimization is done using a simulated annealing scheme with 15 iterations optimizing all the parameters at once. The employed optimization criteria is to measure the shape similarity of the deformed MRI and the full X-ray image. For this purpose we use the dice coefficient to calculate the overlap of the full X-ray mammogram with the projection of the deformed MRI.

A more detailed description of the biomechanical based registration can be found in Hopp et al.<sup>1</sup>

## 2.2 Image based registration

After aligning the MRI to the full X-ray mammogram, an image based registration is implemented as shown in Figure 3 in order to align the full X-ray mammogram to the spot mammogram. Two pre-processing steps are

done before the alignment.

First, a resampling is applied, since spot mammograms have a resolution which may differ from the resolution of the full view mammogram.<sup>11</sup> In our available data, the image resolution of the full view mammogram is 0.05 mm/pixel while the image resolution of the spot mammogram is 0.0488 mm/pixel.

Second, the spot mammogram is rotated by either 90 degrees or 270 degrees, depending on which breast was examined, in order to match the presentation of the breast in the full mammogram.

After pre-processing, the alignment is done using a 2D convolution of the full X-ray mammogram with the spot mammogram. The spot mammogram is considered as a kernel which slides over the full X-ray mammogram, performing an element-wise multiplication and then summing up results into a single output pixel. This matching process allows resolving a translational transformation between both images. We take into consideration to use the spot mammogram at 0° rotation angle to be in the same position of the full X-ray mammogram. Hence, we assume that, although both images have been taken in a different imaging situation as explained before, the deformation state is comparable. The position of the maximum of the convolution is considered as the transformation parameter of the left top corner of the registered image.

### 2.3 Evaluation method

We evaluate the accuracy of our registration methods using annotated lesions in the three modalities as a landmark. The Target Registration Error (TRE) is defined as the Euclidean distance between the center of the predicted lesion in the registered image and the center of the annotated lesion from the radiologist in the unregistered image.

## 3. RESULTS

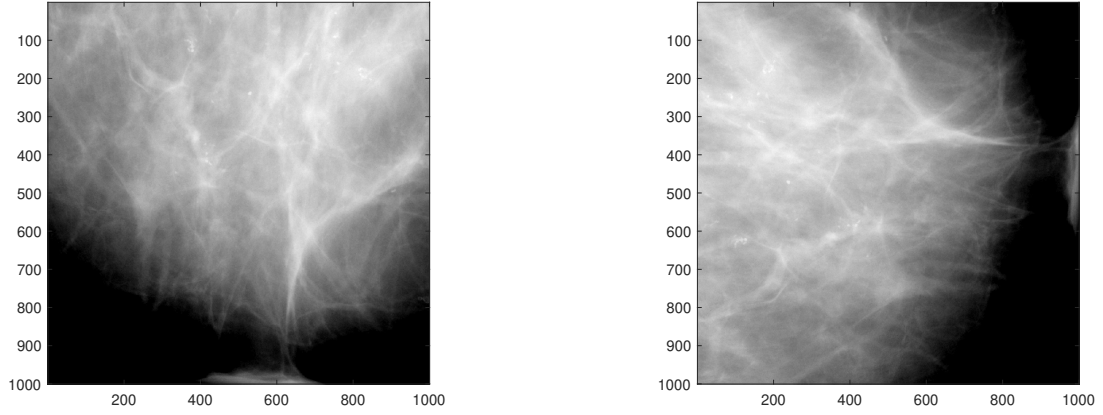
We tested the methods using one patient dataset from the Medical University of Vienna. The dataset consisted of a full set of MRI images taken with and without contrast agent on a Siemens 3T Trio Tim device, a full field digital cranio-caudal view (CC) mammogram taken on a Philips Mammo MicroDose L30 digital mammography device, and a spot view mammogram acquired at a 0° rotation angle of the compression plates taken during X-ray biopsy on a Fischer table. The dataset was selected such that a landmark could be clearly identified by a radiologist in all modalities for evaluation purposes. As a landmark, the circumference of the lesion in the MRI volume is defined by six points, representing the maximal expansion of the lesion in each direction. Accordingly, within the full and spot mammogram, four points representing the maximal expansion of lesion in each direction were acquired from an experienced radiologist as shown in Figure 4. The center point was calculated as the arithmetic mean of these points.

To evaluate the accuracy of the registration we applied two steps: the TRE of landmarks is calculated for each registration step separately compared to the originally annotated lesions by the radiologist in the three modalities. Afterwards, the TRE of both registration steps in combination is calculated based on the predicted lesion position originating from the MRI annotation from the first step. This is given as an input for the second step (image based registration) to predict the position in the spot mammogram image.

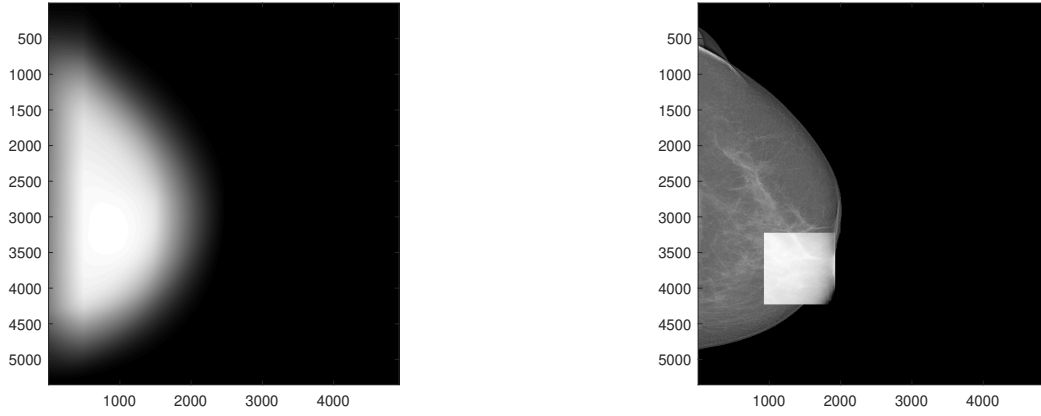
To calculate the TRE of the first processing step, the Euclidean distance between the projected center of the lesion marked in the MRI and the lesion marked in the full X-ray mammogram is measured as shown in equation 1.  $TRE_{Biomechanical}$  is calculated twice; without and with optimization. Before optimization,  $TRE_{Biomechanical}$  using only the empiric standard parameters is 7 mm as shown in (Figure 5 left). After optimization,  $TRE_{Biomechanical}$  has been improved to 2.4 mm as shown in (Figure 6 left). The green dot represents the center of the lesion that was marked by the radiologist and the red dot represents the predicted lesion center from the biomechanical model based registration.

For the second processing step, the displacement of centers of lesions is estimated from the alignment of spot mammogram and full X-ray mammogram images using equation 2 and  $TRE_{Imagebased}$  is 9.5 mm.

In order to calculate the total TRE, the predicted position in the spot mammogram based on the two steps of the registration is compared to the ground truth marking in the spot mammogram.  $TRE_{total}$  is calculated as well before and after optimization.  $TRE_{total}$ , in this case using equation 3 is 4.8 mm as shown in (Figure 5



(a)



(b)

Figure 3. Image based registration in two steps: preprocessing and convolution method. Preprocessing (a): Scaling (first) and rotating (second) of spot mammogram. Convolution method (b): The convoluted image from the full X-ray mammogram and spot mammogram (first). The spot mammogram is aligned with the full X-ray mammogram based on the maximum position of the convolution method (second).

right), while after optimization  $TRE_{total}$  is 7.3 mm as shown in (Figure 6 right). It has been realized that before optimization the  $TRE_{Biomechanical}$  and  $TRE_{Imagebased}$  compensates partly, which results in having a total error of 4.8 mm. However after optimization, our  $TRE_{Biomechanical}$  has been decreased to 2.4 mm, which shows that the  $TRE_{Imagebased}$  has a higher effect on our total error.

$$TRE_{Biomechanical} = \|C_{XR} - C_{MRI}\| \quad (1)$$

$$TRE_{Imagebased} = \|C_{CR} - C_{XR}\| \quad (2)$$

$$TRE_{Total} = \|C_{CR} - C_{CRpredicted}\| \quad (3)$$

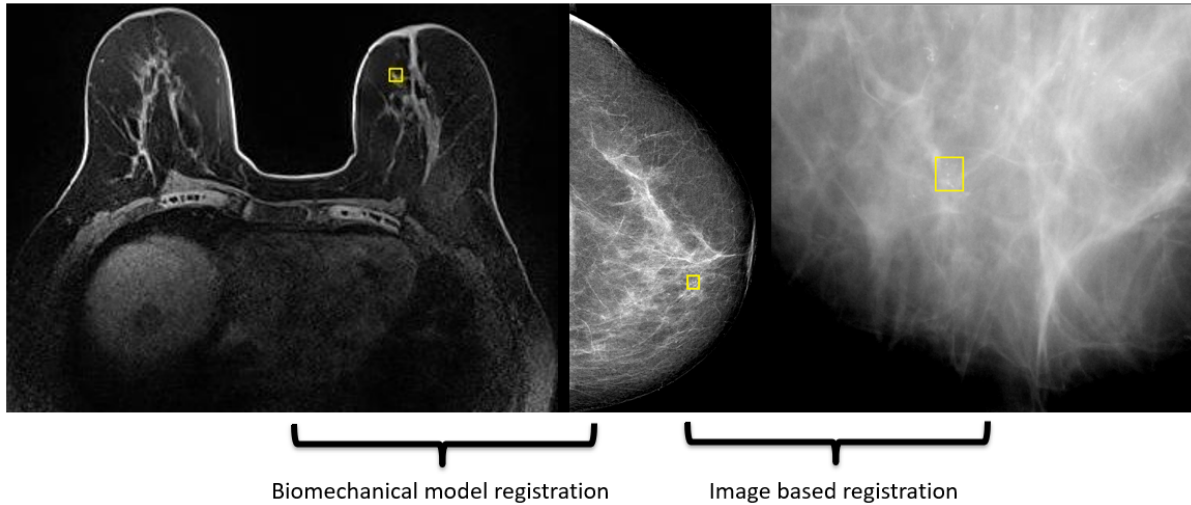


Figure 4. Two step image registration between MRI and spot mammograms for X-ray guided stereotactic breast biopsy. To register MRI (left) with full view mammograms (middle), a biomechanical model based registration is used. To register spot mammograms (right) with full view mammograms (middle), an image based registration is applied. Yellow rectangles indicate the marked lesions in all modalities by an expert radiologist.

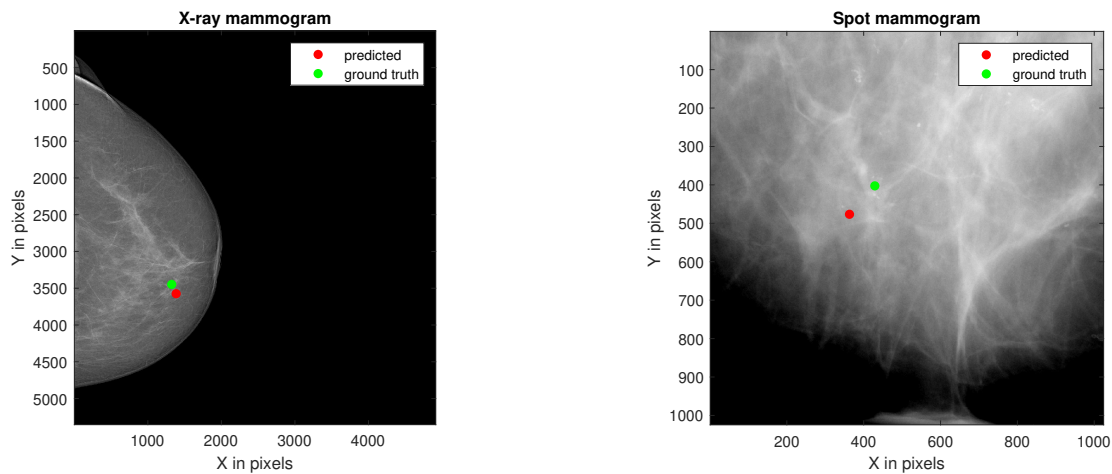


Figure 5. The predicted lesion from the biomechanical model based registration in full X-ray mammograms without optimization (left). The predicted lesion based on the two steps of registration in spot mammogram (right).

#### 4. DISCUSSION AND CONCLUSION

We presented an approach to align MRI volumes with spot mammograms taken during X-ray guided biopsy. To our best knowledge, an image registration between MRI, full X-ray mammograms and spot mammogram for X-ray guided stereotactic breast biopsy has not been presented before. The method is based on two registrations steps: a biomechanical model based and an image based registration. After applying the model based method to virtually compress the MRI, an X-ray like projection is created, which is aligned with the full view mammogram. Afterwards the full view mammogram is aligned with the spot mammogram to deliver spatial correlation with X-ray guided biopsy.

Preliminary results were presented. Though only a small dataset of one patient has been used, our proposed methods provide promising results with a total TRE of 7.3 mm. Since our methods after optimization shows that image based registration has higher effect on our total error we are planning in future to evaluate different

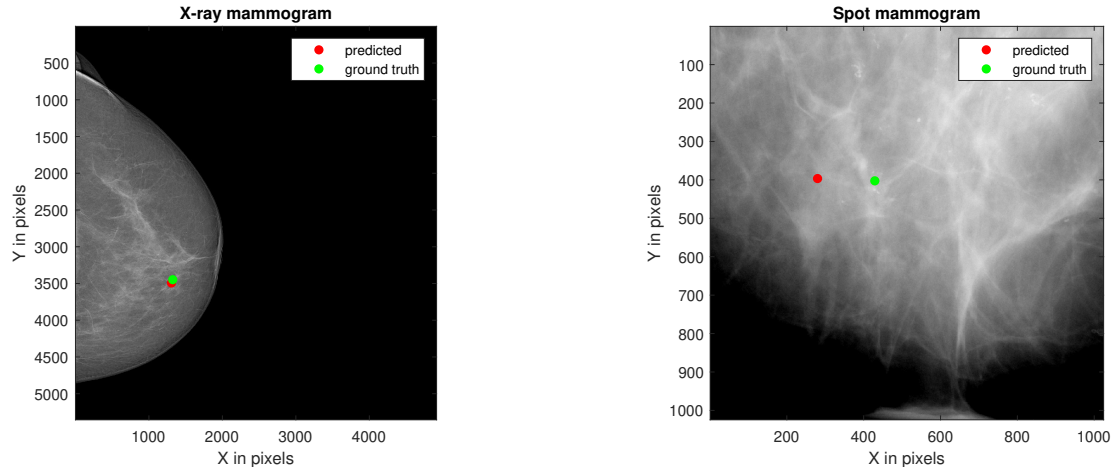


Figure 6. The predicted lesion from the biomechanical model based registration in full X-ray mammograms with optimization (left). The predicted lesion based on the two steps of registration in spot mammogram (right).

deformation models instead of only assuming translational movement.

In future, we will validate the results with more clinical datasets. Also, the influence of the TRE on the proposed workflow will be analyzed in order to answer the question of whether a matching-guided biopsy is possible in a clinical setting. Having such a method would allow performing the broadly available and less expensive X-ray guided biopsy even to a lesion that can only be seen in MRI.

## ACKNOWLEDGMENTS

This work was funded by the German Research Foundation (DFG) under grant number 5565/3-1 and the Austrian Science Fund (FWF) under grant number 4240 .

## REFERENCES

- [1] Hopp, T., Baltzer, P., Dietzel, M., Kaiser, W., and Ruiter, N., “2D/3D image fusion of X-ray mammograms with breast MRI: Visualizing dynamic contrast enhancement in mammograms,” *International journal of computer assisted radiology and surgery* **7**, 339–48 (06 2011).
- [2] “American Cancer Society. Cancer Facts & Figures 2009 Atlanta: American Cancer Society,” (2009).
- [3] <https://www.who.int/cancer/prevention/diagnosis-screening/breast-cancer/en/> (2018).
- [4] Houssami, N., Ciatto, S., Macaskill, P., Lord, S. J., Warren, R. M., Dixon, J. M., and Irwig, L., “Accuracy and surgical impact of magnetic resonance imaging in breast cancer staging: Systematic review and meta-analysis in detection of multifocal and multicentric cancer,” *Journal of Clinical Oncology* **26**(19), 3248–3258 (2008). PMID: 18474876.
- [5] Mann, R., Balleyguier, C., Baltzer, P., Bick, U., Colin, C., Cornford, E., Evans, A., Fallenberg, E., Forrai, G., Fuchsjäger, M., Gilbert, F., Helbich, T., Heywang-Köbrunner, S., Herrero, J., Kuhl, C., Martincich, L., Pediconi, F., Panizza, P., Pina, L., and Sardanelli, F., “Breast MRI: Eusobi recommendations for women’s information,” *European radiology* **25** (05 2015).
- [6] Spick, C. and Baltzer, P. A. T., “Diagnostic utility of second-look US for breast lesions identified at MR imaging: Systematic review and meta-analysis,” *Radiology* **273**(2), 401–409 (2014).
- [7] Clauser, P., Mann, R., Athanasiou, A., Prosch, H., Pinker, K., Dietzel, M., Helbich, T. H., Fuchsjäger, M., Camps-Herrero, J., Sardanelli, F., Forrai, G., and Baltzer, P. A. T., “A survey by the european society of breast imaging on the utilisation of breast MRI in clinical practice,” *European radiology* **28**, 1909–1918 (May 2018).

- [8] Kuhl, C. K., Strobel, K., Bieling, H., Wardelmann, E., Kuhn, W., Maass, N., and Schradling, S., “Impact of preoperative breast MR imaging and MR-guided surgery on diagnosis and surgical outcome of women with invasive breast cancer with and without dcis component,” *Radiology* **284**(3), 645–655 (2017).
- [9] Ruiter, N. V., Stotzka, R., Muller, T., Gemmeke, H., Reichenbach, J. R., and Kaiser, W. A., “Model-based registration of X-ray mammograms and MR images of the female breast,” *IEEE Transactions on Nuclear Science* **53**(1), 204–211 (2006).
- [10] Hopp, T., Dietzel, M., Baltzer, P., Kreisel, P., Kaiser, W., Gemmeke, H., and Ruiter, N., “Automatic multi-modal 2D/3D breast image registration using biomechanical FEM models and intensity-based optimization,” *Medical Image Analysis* **17**(2), 209 – 218 (2013).
- [11] Carr, J. J., Hemler, P. F., Halford, P. W., Freimanis, R. I., Choplin, R. H., and Chen, M. Y. M., “Stereotactic localization of breast lesions: How it works and methods to improve accuracy,” *RadioGraphics* **21**(2), 463–473 (2001). PMID: 11259709.
- [12] Wu, S., Weinstein, S., Keller, B. M., Conant, E. F., and Kontos, D., “Fully-automated fibroglandular tissue segmentation in breast MRI,” in [*Breast Imaging*], Maidment, A. D. A., Bakic, P. R., and Gavenonis, S., eds., 244–251, Springer Berlin Heidelberg, Berlin, Heidelberg (2012).
- [13] Kannan, S., Ramathilagam, S., Devi, R., and Sathya, A., “Robust kernel FCM in segmentation of breast medical images,” *Expert Systems with Applications* **38**(4), 4382 – 4389 (2011).
- [14] Fang, Q. and Boas, D. A., “Tetrahedral mesh generation from volumetric binary and gray-scale images,” in [*Proceedings of the Sixth IEEE International Conference on Symposium on Biomedical Imaging: From Nano to Macro*], *ISBI’09*, 1142–1145, IEEE Press (2009).
- [15] Wellman, P., Howe, R., and Kern, K., “Breast tissue stiffness in compression is correlated to histological diagnosis,” (1999).
- [16] Smole, P. C., Kaiser, C., Krammer, J., Ruiter, N. V., and Hopp, T., “A comparison of biomechanical models for MRI to digital breast tomosynthesis 3D registration,” in [*Computational Biomechanics for Medicine*], Nielsen, P. M. F., Wittek, A., Miller, K., Doyle, B., Joldes, G. R., and Nash, M. P., eds., 107–117, Springer International Publishing, Cham (2019).
- [17] Smith, M., [*ABAQUS/Standard User’s Manual, Version 6.9*], Dassault Systèmes Simulia Corp, United States (2009).
- [18] Waade, G. G., Highnam, R., Hauge, I. H. R., McEntee, M. F., Hofvind, S., Denton, E., Kelly, J., Sarwar, J. J., and Hogg, P., “Impact of errors in recorded compressed breast thickness measurements on volumetric density classification using volpara v1.5.0 software,” *Medical Physics* **43**(6Part1), 2870–2876 (2016).